Phenol removal from water in the presence of nano-TiO₂ and a natural activated carbon: intensive and extensive processes

H. Belayachi[1, *], F. Nemchi[1], A. Belayachi[1], S. Bourahla[1], M. Belhakem[1]

[1]Laboratoire de Structure, Élaboration et Application des MatériauxMoléculaires (SEA2M), Faculté des Sciences Exactes et de l'Informatique (FSEI), Université Abdelhamid Benbadis-Mostaganem, Algérie

*Corresponding author: hanane.belayachi@univ-mosta.dz; Tel.: +21345 36 64 72; Fax: +213 45 36 64 73

ARTICLE INFO

ABSTRACT/RESUME

Abstract: *In this work two photocatalytic processes for the degradation of phenol in water are presented. The first one is extensive (EP) which carried out in a treatment chain of two steps allowing the adsorption of the pollutant by a natural activated carbon from the grapes. This operation is followed by a photocatalytic degradation of the residual phenol in the presence of TiO₂. The second process is intensive (IP) is realized in one step in the presence of a hybrid photacalyticnano material prepared from a natural activated carbon and TiO₂.*

The evaluation of the two processes, EP and IP, is based on the analytical monitoring of the initial and final parameters of the water to be treated, i.e., the phenol concentration by liquid phase chromatography (HPLC) and total organic carbon (TOC). For both processes, the sampling carried out every 10 min for 120 min of treatment time to measure the phenol concentrations.

The elimination and degradation rates in the case of the intensive process are better than the extensive process. In both processes, the catechol molecule was detected as an under product of degradation. However, for the IP process, the concentration of this by-product of phenol was insignificant in the EP process.

I. Introduction

Phenolic compounds belong to organic pollutants, which are widely distributed in the environment. They may be present in waste waters and natural environmental waters. Phenols are introduced to the environment in variety of ways like wastes from paper manufacturing, agriculture, petrochemical industry, coal processing or as pharmaceutical wastes [1, 2].

According to the EU directive, maximum concentration of total phenols in drinking water is 0.5 μg L^{-1}, while individual phenol concentrations should be under 0.1 μg L^{-1} [3].

After entering into the fish body, phenol affects the metabolism, survival and growth and reproductive potential of fish. For aquatic ecosystem, phytoplankton and zooplankton populations are affected in the presence of a micro-concentration of phenol by the reduction of the limnological parameters [4].

Several processes have been used to eliminate phenolic compounds, conventional processes as coagulation-flocculation treatment and adsorption are effective in wastewater treatment but they only transfer the contaminants from water to solid creating considerable quantities of chemical sludge that are difficult to manage [5].

Actually, an emerging technology based on the oxidation of organic compounds, by the use of advanced oxidation processes (AOPs). The AOPs are based on the generation of hydroxyl radicals

(˙OH) which are the principal agents able to degrade several organic contaminants. This species is a powerful oxidant with an oxydoreduction potential E°($^{\bullet}OH/H_2O$)=2.85 V/NHE [6]. This radical is a powerful and not selective oxidant toward the organic compounds with a rate constant beyond 10^6 (mol/L)$^{-1}$ s^{-1} [6,7]. Different techniques are used to generate the hydroxyl radicals such as: ozone with ultraviolet light [7], hydrogen peroxide with ultraviolet light and photocatalysis [8,9], which uses a semi-conductor under UV radiations. Photocatalytic oxidation in the presence of titanium dioxide has been investigated in more detail during the past decade. The use of TiO_2 particles has been of enormous attention due to its efficiency non-toxicity, high activity, photochemical inertness and low cost [10].

To treat wastewater containing phenol molecules, adsorption process seems to be the best method but in reality it can only concentrate phenol in a denser medium than water [11]. On the other hand, photocatalysis in the presence of TiO_2 makes it possible to degrade the pollutant in situ but requires a significant energy contribution. The conciliation of the two methods was the subject of this work with two different approaches:

(i) an extensive process (EP) including an adsorption in the presence of a natural activated carbon then heterogeneous photocatalysis with TiO_2 nanoparticles;

(ii) an intensive process (IP) which is a photocatalytic process with a hybrid material made of a natural activated carbon and TiO_2 nanoparticles.

A comparative study between the two methods was conducted on the basis of analytical methods including chromatography and total organic carbon measure.

II. Materials and methods
II. 1 Reagents
Distilled water was used to prepare the synthetic aqueous solutions. Phenol, hydroquinone, catechol, p-benzoquinone and acetonirile were purchased from ALDRICH with purities of 99.8% and were of analytical grades.

II.2 Materials
- Photocatalyst: The TiO_2 nanoparticules from Sigma–Aldrich with the physical characteristics: 99.7% on a trace metal basis, 25 nm particle size and surface area of 220 m^2 g^{-1}, was used as received in this study. It was mainly composed of Anatase phase.
    - Natural activated carbon (NAC) preparation: natural grape marc as a raw material provided from SidiM'HamedBenali cavern (North of Algeria) was used as precursor for activated carbon preparation. Grape marc was washed several times with distilled water and dried at

100°C during 24 h, then crushed and sieved to obtain particle diameter between 0.5 and 1 mm. The resulting material was then impregnated in diluted phosphoric acid solution (40%) and heated at 170°C for 2 h, then filtered and then dried during 24 h at 110°C. After this operation, a thermic activation was done at 600°C for 3 h. The obtained nanomaterial was washed with hydrochloric acid solution (0.1 M), followed by repeated washing with distilled water until negative test by lead acetate saturated aqueous solution. The prepared activated carbon was dried at 100°C for 24 h and sieved to obtain a particle size < 0.07 mm.

- Hybrid nanomaterial (NAC-TiO_2):
The composite NAC-TiO_2 was prepared by stirring mechanically 10 g of NAC and 1 g of TiO_2 in 100 mL of H_3PO_4 (1 M) during 24 h. A Centrifugation was done to separate liquid and solid phases. The solid fraction was then washed with distilled water until achieve the neutral pH and the disappearance of phosphate ions using a mixture of aqueous solution of concentrated nitric acid and ammonium molybdate reagent. A closed-loop washing for 2 h using ethanol and drying at 105°C were applied to obtain a homogenous hybrid.

II. 3 Materials characterization
The surface area and macropore surface area were respectively estimated by BET and t-plot method. The pore size distribution was determined by BJH method. The FTIR spectra of the three materials were done by the pressed-disk method with potassium bromide on Shimadzu FTIR spectrometer.

II. 4 Process apparatus
Two experimental devices were used. The first one describes the extensive process (Fig. 1a) and the second presents the intensive process (Fig. 1b).

The UV lamp used is Philips brand and type TLD 18W / 08, having an electric power of 18 Watt, emitting a light between 350 nm and 390 nm with a maximum at 365 nm. In these processes, the tanks of a volumic capacity of 0.5 L, are mechanically stirred and operate in an open space to approach the configuration of a wastewater treatment plant.

II.5 Procedure
- Extensive process (EP): two materials were tested, i.e., the natural activated carbon (NAC) was used in the first thank and TiO_2 in the second one. In the first chamber an amount was added to a phenol aqueous solution (100 μM) to form a suspension dose of 2 g L^{-1} in NAC adsorbent. When the equilibrium adsorption is reached, the suspension was centrifuged to separate water from the solid particles.
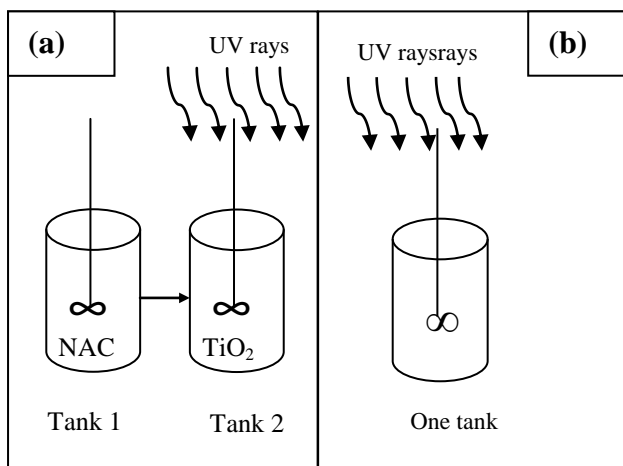
Figure 1. *Process treatments: (a) Extensive, (b) Intensive*

- Intensive process (IP): the hybrid nanomaterial (NAC-TiO$_2$) was used in a single step. The material was added to the phenol solution (100 μM) to obtain a suspension with a dose of 2 g L^{-1} of the photocatalyst hybrid. Before exposing the mixture to UV irradiations, the suspension was stirred during 15 min in the darkness in order to reach the adsorption equilibrium. The samples to be analyzed were taken every 10 min for a treatment time of 120 min and were centrifuged to eliminate the NAC-TiO$_2$ particles.

The doses of 2 g L^{-1} of NAC and TiO$_2$ were chosen so that there is the same amount of particles in both processes. This will allow to compare the performance of the two processes under the same conditions. In IP and EP processes, the adsorption equilibrium was estimated when the elimination rate slowed down as a function of time.

For the optimization of the two processes, different doses of NAC and TiO$_2$ were applied, i.e., 0.1, 0.5, 1, 1.5 and 2 g L^{-1}.

The removal of phenol in water was followed by high performance liquid chromatography (HPLC). The equipment is equipped with a C-18 column reversed phase and UV/Vis/PDA detector that the wavelengths range is [190 - 900 nm].

The wavelength was fixed at 254 nm in all manipulations. The mobile phase is formed by a mixture of water-acetonitrile system (V/V: 40/60). The elution was done in isocratic mode with a flowrate of 1 mL min^{-1}.

For the kinetic study, a sample of volume equal to 5 mL was taken every 10 min to be centrifuged to separate solid particles from water. After, the supernatant was analyzed by HPLC and TOC-meter.

All experiments were conducted in natural pH of 5.1 and ambient temperature of 25°C. The electrical power of the UV source (365 nm) is 18 Watt.

The elimination rate was calculated by the following equation:

$$Elimination\ rate\ (\%) = \frac{c_i - c_f}{c_i} \times 100 \qquad (1)$$

Where, C_i and C_f are the initial and the final phenol concentrations, respectively.

The degradation was determined by the total organic carbon (TOC) using the calibrated IC method by a potassium phthalate aqueous solution. The degradation rate was evaluated by the following equation:

$$Degradation\ rate\ (\%) = \frac{TOC_i - TOC_f}{TOC_i} \times 100 \qquad (2)$$

Where, TOC_i and TOC_f are the initial and the final TOC, respectively.

The TOC is a global parameter which provides information on the concentration of phenol and the product's degradation.

III. Results and discussion
III.1 Material characterizations
III.1.1 Nitrogen adsorption isotherm
The analysis of the adsorption/desorption isotherms provides information on the porous texture of the materials with adsorptive and/or photocatalytic applications. The most important conclusions tired from this analytical technique are the specific surface and the porous distribution. The B.E.T isotherms of the three materials NAC, TiO$_2$ and NAC-TiO$_2$ are presented in figure 2.a.

For the three materials, it is visible that desorption does not match with the adsorption. Isotherms are consequently categorized as type IV of the IUPAC classification [12] with the characteristic of mesoporous solids [13].

In this case, the adsorption takes place at low relative pressure, then at high relative pressure. Hystereses are characteristic of solids with cylindrical channels or formed of spherical aggregates and/or agglomerates with uniformity of the pores [14].
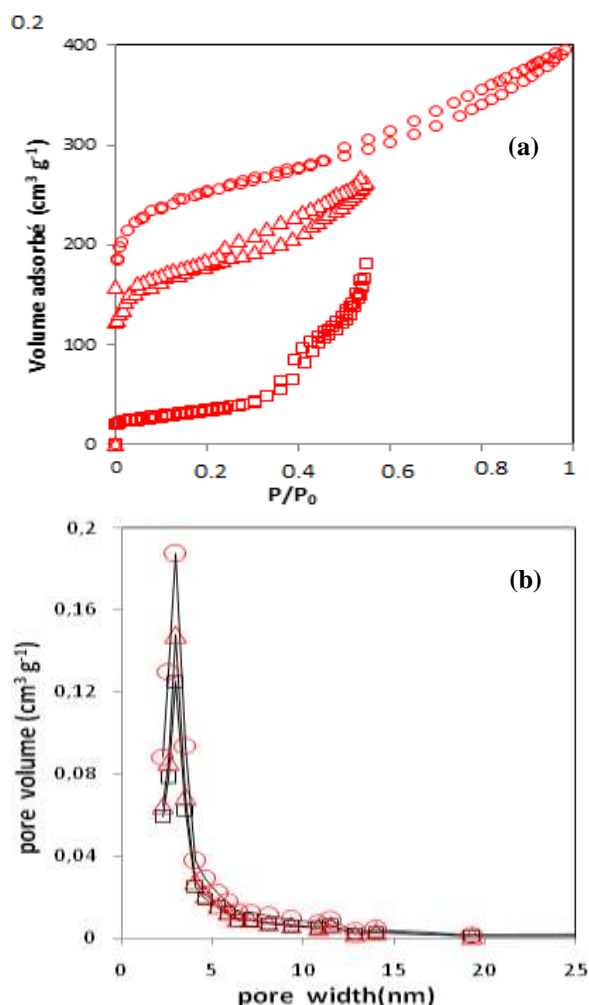
Figure 2. *(a) N$_2$ adsorption–desorption isotherms, (b) Pore size distributions of: (□) TiO$_2$, (Δ) NAC-TiO$_2$ and (○) NAC*

Table 1 summarizes the specific surfaces as well as those of a certain number of textural characteristics, such as the total volume of the pores, the volume of the micropores and the area of the external surface, determined by the Harkins-Jura method, called also t-plot method. The latter is particularly interesting for discriminating in the volumes of nitrogen adsorbed the part corresponding to the adsorption inside the micropores. The volume of the mesopores and the distribution of the pore size were calculated using the equation of the Barrett-Joyner-Halenda method which is applied in the case of mesoporous solids, the results are illustrated in figure 2.b. The pore size distributions corroborate the mesoporosity of nanoparticles whose diameter is between 2 and 12 nm. The appropriate activation method made it possible to obtain a specific surface area (available for nitrogen) of 1205 m^{2}g^{-1} for the NAC, which is very significant. This large specific surface area makes it possible to obtain a highly dispersed active phase and to improve the interparticle diffusion of the adsorption phase.

When the TiO$_2$ particles are introduced in NAC structure, we have noticed a little decrease in surface area and pore volume. This can be explained by the fact that the TiO$_2$ particles settle inside the pores and occupy sites inside and outside the available surface. However, the NAC-TiO$_2$ remains a hybrid material with high adsorptive properties and a photocatalytic activity which the intensity will be presented later in this article.

Table1. *BET-BJH analysis*

	S$_{BET}$ (m^2 g^{-1})	S$_{externe, t-plot}$(m^2 g^{-1})	V$_{meso}$ (cm^3 g^{-1})	V$_{micro}$ (cm^3 g^{-1})
TiO$_2$	119	107	0.300	0.006
NAC	1205	776	0.409	0.309
NAC-TiO$_2$	1010	351	0.327	0.300

III.1.2 FTIR analysis

The FTIR spectra of the three composite materials are shown in Fig. 3. In the TiO$_2$ and/or NAC-TiO$_2$ spectra, it can be seen that a large peak between 500 and 760 cm^{-1} is attributed to the asymmetric stretching vibration of Ti–O–Ti bond, whereas the peaks at 1620 cm^{-1} is corresponding to the bending vibration of O–H bond of the chemisorbed H$_2$O [15]. Concerning the peaks around 3500 cm^{-1}, it is assigned to the stretching mode of O–H bond and is related to the free water present in the structure of TiO$_2$ [16]. Therefore, we can say that TiO$_2$ particles are present in the NAC-TiO$_2$ hybrid.

The presence of activated carbon is frequently indicated by one absorption peak and three absorption bands [17]:

(i) two bands around 3430 and 1610 cm^{-1} attributed to the stretch and bend vibrations of O-H, respectively,

(ii) (ii) one peak at 1420 cm^{-1} and (iii) one band at 1065 cm^{-1} due to skeleton vibration.

The spectra of NAC-TiO$_2$ material also show a strong band at 1610-1570 cm^{-1} due to the C–C vibrations in aromatic rings. The bands at 880, 835, and 775 cm^{-1} are due to the out-of-plane deformation mode of C–H for substituted benzene rings [16]. Consequently, it is right to confirm the hybrid character of the NAC-TiO$_2$.
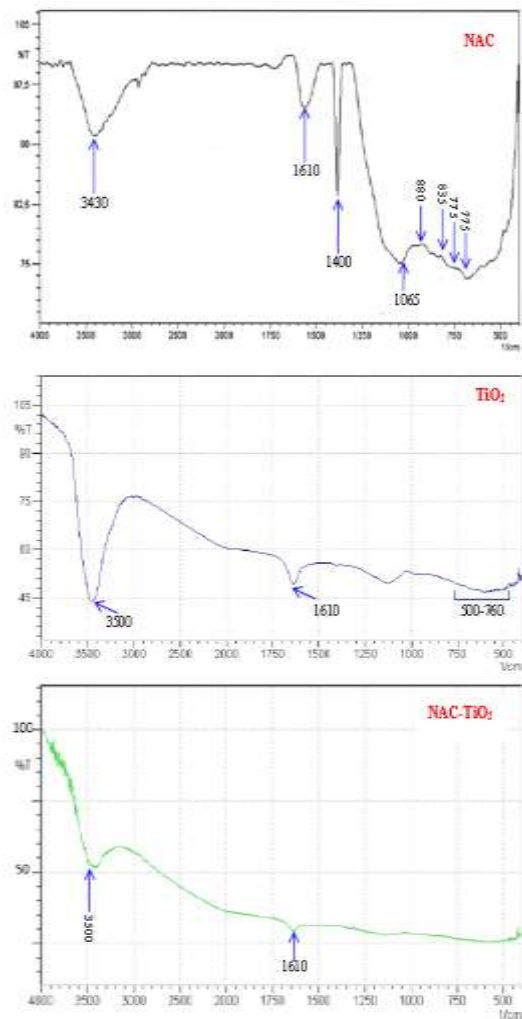
Figure 3. *FTIR spectra of natural activated carbon (NAC), TiO₂ and hybrid (NAC-TiO₂)*

III.2 Phenol solution treatment
III.2.1 Extensive process (EP)

Figure 4 shows the kinetics of phenol elimination in the extensive process. The concentration of phenol decreases in the first tank of activated carbon and continues the same tendency in the second one in the presence of titanium oxide. The addition of the adsorbent agent (NCA) and the photocatalyst (TiO₂) successively in the two tanks has improved this tendency.
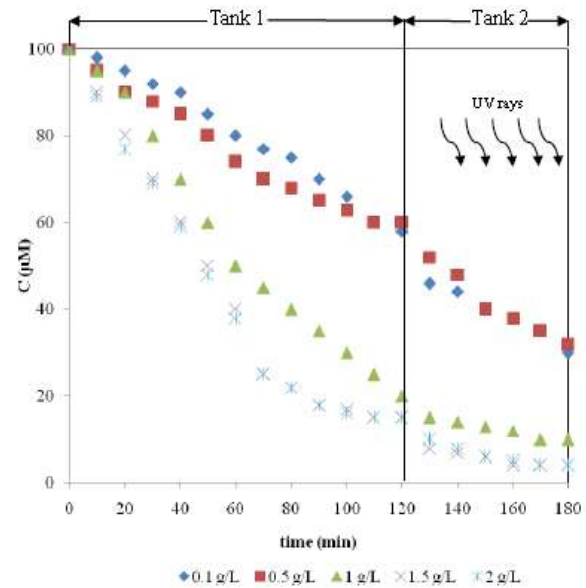
Figure 4. *Kinetic phenol (100 μM) elimination in extensive process for different NAC and TiO₂ doses (natural pH = 5.1, temperature = 25°C and power UV light (365 nm) = 18 watts)*

Quantitatively, the doses of 0.1 and 0.5 g L^{-1} almost cause the same elimination rate of phenol (~ 70%). This rate is substantially improved with doses of 1.5 and 2 g L^{-1} to reach 96%.

The large specific surface and the availability of active carbon active sites push the phenol molecules to migrate towards the pores of the adsorbent to settle there. The residual pollutant molecules are then eliminated by TiO₂ particles by another mechanism different from that of NCA. Indeed, in the first stage the phenol is removed by adsorption process, where the molecules are transferred from the liquid phase to the solid phase [18,19]. The rest of the molecules are then degraded by photocatalysis process in the presence of TiO₂. Figure 5 shows the chromatographs and TOC values of phenol before and after treatment. We can see the veracity of the last interpretations, i.e., an extensive process established over two stages: adsorption then photocatalysis. In the first tank, place of adsorption, the chromatographic peak of phenol decreases by 70% without the appearance of intermediate compounds. In the same context, the TOC has decreased to 49 ppm which corresponds to 33.8% of organic pollution elimination rate.
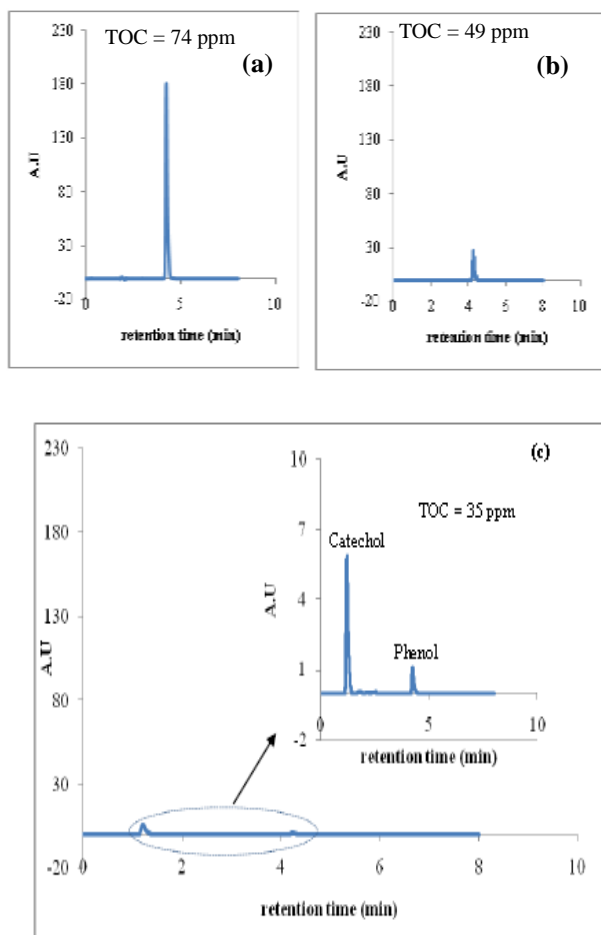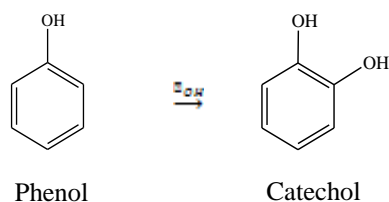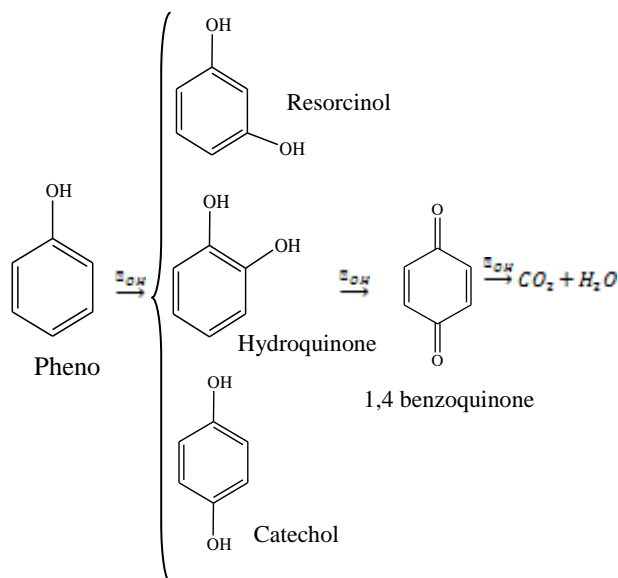
The other compounds such as hydroquinone and p-benzoquinone were not detected as under products. This can be explained by the instantaneous character of the photocatalytic reaction. However, it exists analytical technics more adapted to identify under-products of degradation using chromatography coupled to mass spectroscopy (GC-MS or LC-MS). In this case, it is possible to see other compounds during the degradation process according the following mechanism [19, 20]:

Figure 5. *Phenol (100 μM) chromatogram in extensive process (EP): (a) untreated phenol (0 min), (b) treated phenol by NAC (2 g L^{-1}) in tank 1 (120 min) and (c) treated residual phenol by TiO$_2$ (2 g L^{-1}) in tank 2 (60 min) (natural pH = 5.1, temperature = 25°C and power UV light (365 nm) = 18 watts)*

This proves the operation of pollutant transfer from the water to activated carbon without mineralization. In the second tank, place of photocatalysis, the chromatographic peak of phenol decreases more 70% to achieve 96% with the appearance of a degradation product. In parallel and to identify the chromatograph peak at the retention time of 1.2 min, an injection of some standards of organic compounds has revealed the presence of catechol as only under product of degradation according the following reaction:


The availability of OH radicals can lead to the formation of mesomers such as Resorcinol and Hydroquinone. The photoreaction can continue in favor of the formation of 1,4 benzoquinone and the opening of the aromatic ring of the latter for complete mineralization (CO$_2$+H$_2$O).

UV light excites the surface of TiO$_2$ to release the OH radicals which attack the phenol molecules in favor of the appearance of catechol which is known to be more biodegradable than the initial molecule. The opening of the benzene cycle is easier in the case of catechol than that of phenol [20]. The TOC value falling from 74 ppm to 35 ppm, corresponding to 52.7% of degradation rate, confirms this aspect of molecular degradation of phenol in the presence of TiO$_2$ particles.

III.2.2 Intensive process (IP)

Figure 6 shows the kinetic of elimination of phenol in the presence of the NAC-TiO$_2$ hybrid at different
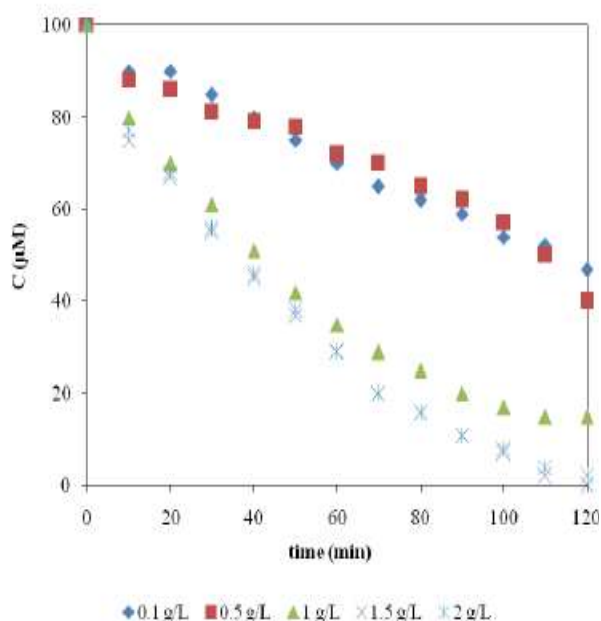
doses. The intensive process gives a total elimination of phenol in the presence of 1.5 g L^{-1} of hybrid photocatalyst. The increase of the dose to 2 g L^{-1} causes a slight decrease in the elimination rate (98%). This is due to the screen effect of solid particles which avoid the penetration of UV light into solution. To confirm the degradation process, we have examined the sample treated during 90 min when 1.5 g L^{-1} of NCA-TiO$_2$ is used.

Figure 6. Kinetic phenol (100 μM) elimination in intensive process for different NAC-TiO$_2$ hybrid doses (natural pH = 5.1, temperature = 25°C and power UV light (365 nm) = 18 watts)

It can be seen in figure 7 that the decrease of the phenol peak was in favor of the appearance of another peak attributed to catechol compound with a lower concentration compared to the extensive process.

The degradation rate in this case was of 89.2% against 52.7% obtained by the extensive process. This high mineralization rate suggests that phenol has been converted to CO$_2$ and H$_2$O and catechol residues. Usually, photocatalytic reaction is initiated by the formation of phenoxyl radicals after the electron transfer. Further reaction leads to the formation of benzoquinone compound. The reaction continues until breakage of the benzene ring that produces various organic acids as maleic acid, malonic acid, acetic acid and oxalic acid [21,22]. In this context, it is interesting to remember that the

biodegradability of these under product compounds is significantly better than the phenol [24].

At this stage of the study, it can be supposed that the intensive process is more effective than the extensive process. This can be explained by two evident reasons [25, 26]:

(i) The transfer of the phenol molecule from water to the surface of TiO$_2$ is realized by simple gradient of concentration in the case of extensive process;

(ii) The same transfer is promoted by the adsorptive properties of activated carbon in the case of intensive process.

The fact that the hybrid material (NAC-TiO$_2$) is relatively more efficient in terms of decontamination was predictable if we come back to the results of the physicochemical characterization of the three materials.
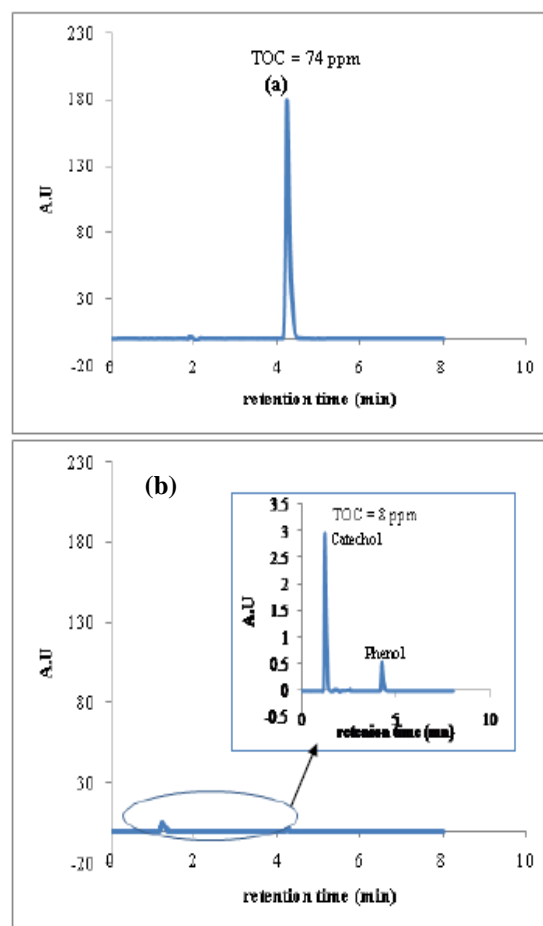

Figure 7. Phenol (100 μM) chromatogram in intensive process (IP): (a) untreated phenol, (b) treated phenol by NAC-TiO$_2$ (time = 90 min, dose = 1.5 g L^{-1}, natural pH = 5.1, temperature = 25°C and power UV light (365 nm) = 18 watts)

Indeed, the identification of C-H and C-C bands by FTIR confirms the organophilic character of the

hybrid material [27, 28], which facilitates the migration of organic compounds such as phenol.

The specific surface area of the order of 1010 m^2 g^{-1}, measured by BET, facilitates first of all this migration to the external surface (351 m^2 g^{-1}) to finally settle in the meso and micropores. Once installed, the phenol molecule can eventually be degraded by radical OH generated by the TiO_2 particles incorporated into the activated carbon [29, 30]. The adsorption-degradation duality is more efficient than the two separate processes since it is possible to degrade a pollutant inside carbon and therefore liberate more pores to introduce other molecules. This may look like a self-regeneration which does not require a downstream operation such as chemical attack and/or combustion, which in some cases can be quite expensive.

IV. Conclusion

This study focuses on the decontamination of water containing recalcitrant organic compounds. It presents the extensive and intensive combinations of adsorption and heterogeneous photocatalysis.

The extensive process is carried out using natural activated carbon in a first stirred tank which is the site of adsorption. The second tank receives the residual pollutant load in the presence of TiO_2 and UV light for a photocatalytic treatment.

The intensive process, in the presence of UV light, is carried out in a single stirred tank in the presence of a hybrid material consisting of natural activated carbon and TiO_2.

Analyses by chromatography (HPLC) and total organic carbon (COT) show the superiority of the intensive process.

The two processes can be extrapolated to a larger geometric scale to be placed in an open-air wastewater treatment plant.

V. Acknowledgment

VI. References

1. Rui Martins, C. ; Rosa Quinta-Ferreira, M. Remediation of *phenolic* wastewaters by advanced oxidation processes (*AOPs*) at ambient conditions: Comparative studies. *Chemical. Engineering. Science* 66 (2011) 3243-3250.
2. Suzuki, H, S.; Araki Yamamoto, H. Evaluation of advanced oxidation processes (AOP) using O_3, UV, and TiO_2 for the degradation of phenol in water. *Journal of Water Progress Engeneering* 7 (2015) 54-60.
3. Kochana, J.; Adamski, J.; Parczewski1, Z. A critical view on the phenol index as a measure of phenol compounds content in waters. Application of a biosensor. Ecological. *Chemical Engineering journal* 19(3) (2012) 383-391.
4. Saha, N.C.; Bhunia, F.; Kaviraj, A. Toxicity of Phenol to Fish and Aquatic Ecosystems. Bull. *Environmental Contamination and Toxicology* 63 (1999) 195-202.
5. Gimeno, O.; Carbajo, M.; Beltrán, F. J.; Javier Rivas, F.Phenol and substituted phenols AOPs remediation,. *Journal of Hazardous Materials* 119 (2004) 99-108.
6. Gonzalez, M. C.; Braun, A. M. VUV photolysis of aqueous solutions of nitrate and nitrite. *Research on Chemical.Intermediates* 21 (1995) 837−859.
7. Zhang, Y.; Zhou, L.; Zeng, C.Q.; Wang, Z.; Gao, SA.; Ji, Y.; Yang, X. Photoreactivity of hydroxylated multi-walled carbon nanotubes and its effects on the photodegradation of atenolol in water.*Chemosphere Journal* 93 (2013)1747–1754.
8. Malvestiti, J. A.; Dantas, R.F. Disinfection of secondary effluents by O_3, O_3/H_2O_2 and UV/H_2O_2: Influence of carbonate, nitrate, industrial contaminants and regrowth. *Journal of Environmental Chemical* Engineering6 (2018) 560-567.
9. Lu, G.; J. Hu. Effect of alpha-hydroxy acids on transformation products formation and degradation mechanisms of carbamazepine by UV/H_2O_2 processSci. *Science of the Total Environment.* 6891 (2019) 70-78.
10. He, H.; Ji, Q.; Gao, Z.; Yang, S.; Zhang, L. Degradation of tri(2-chloroisopropyl) phosphate by the *UV*/H2O2 system: Kinetics, mechanisms and toxicity evaluation. *Chemosphere Journal* 236 (2019) 124388.
11. Umer, M.; Tahir, M.; Usman Azam, M.; Tahir, B.; Alias, H. Montmorillonite dispersed single wall carbon nanotubes (SWCNTs)/TiO_2 heterojunction composite for enhanced dynamic photocatalytic H_2 production under visible light. *Applied. Clay Science* 17415 (2019) 110-119.
12. D. Mc Naught, A.; Wilkinson, A. IUPAC. Compendium of Chemical Terminology, 2nd ed. (the "Gold Book"). Compiled by Blackwell Scientific Publications, Oxford (1997).
13. Díez, E.; Gómez, J.M.; Rodríguez, A.; Bernabé, I.; Sáez, P.; Galán, J. A new mesoporous activated carbon as potential adsorbent for effective indium removal from aqueous solutions. *Microporous and Mesoporous Materials* 295(2020) 109984.
14. Leofanti, G.M.; Padovan, G.; Tozzola, B.; Venturelli, V. Surface area and pore texture of catalysts, *Catalysis Today* 41 (1998) 207-219.
15. Akhter, M.S.; Keifer, J.R.; Chughtai, A.R.; Smith D.M. The absorption band at 1590 cm^{-1} in the infrared spectrum of carbons. *Carbon* 23 (1985) 589–591.
16. Xu, S.; Ng, J.; Zhang, X.; Bai, H.; Delai-Sun D. Adsorption and photocatalytic degradation of Acid Orange 7 over hydrothermally synthesized mesoporous TiO_2 nanotube. *Colloids and Surfaces. A* 379 (2011)169–175.
17. Liu, S.X.; Chen, X.Y.; Chen, X. A TiO_2/AC composite photocatalyst with high activity and easy separation prepared by a hydrothermal method, *Journal of Hazardous Materials* 143 (2007)143-263.
18. Konstantinou, I.K.; Triantafyllos, A.A. TiO_2-Assisted Photocatalytic Degradation of Azo Dyes in Aqueous Solution: Kinetic and Mechanistic Investigations: A Review. *Applied. Catalysis B* 49 (2004) 1–14.
19. Guillard, C.; Lachheb, H.; Houas, A. Influence of chemical structure of dyes, of pH and of inorganic salts on their photocatalytic degradation by TiO_2 comparison of the efficiency of powder and supported TiO_2, *Journal of Photochemistry and Photobiology A* 158 (2003) 27–36.
20. Bandara, J.; Morrison, C.; Kiwi, J. Degradation/decoloration of concentrated solutions of Orange II. Kinetics and quantum yield for sunlight induced reactions via Fenton type reagents. *Journal of Photochemistry and Photobiology A* 99 (1999) 57–66.

21. Cao, J.; Wei, L.; Huang, Q.; Han. Reducing, S degradation of azo dye by zero-valent iron in aqueous solution, *Chemosphere Journal*38 (1999) 565–571.

22. Ahmed, S.; Rasul, M.G.; Martens, W.N.; Brown, R.; Hashib, M.A. Heterogeneous photocatalytic degradation of phenols in wastewater: a review on current status and developments. *Desalination*261 (2010) 3–18.

23. Li, X-y.; Cui, Y-h.; Feng, Y-j.; Xie, Z-m.; Gu, J-D. Reaction pathways and mechanisms of the electrochemical degradation of phenol on different electrodes. *Water Research*39 (2005) 1972–1981.

24. M'Arimi, M.M.; Mecha, C.A.; Kiprop, A.K.; Ramkat, R. Recent trends in applications of advanced oxidation processes (AOPs) in bioenergy production: Review, *Renewable and. Sustainable Energy Reviews121 (2020) 109669.*

25. Rodrıguez-Gonzalez, V.; Alfaro, S. O.; Torres-Martınez, L. M.; Cho, H. S.; Lee, S.W. Silver-TiO_2 nanocomposites: synthesis and harmful algae bloom UV-photo-elimination. *Applied.Catalysis. B: Environmental* 98 (2010) 229-234.

26. Yu, J. G.; Yu, H. G.; Cheng, B.; Zhou, M.; Zhao, X. Enhanced photocatalytic activity of TiO2 powder (P25) by hydrothermal treatment. *Journal of Molecular Catalysis A: Chemical*253 (2006) 112–118.

27. Dionysiou, D.; Suidan, M.; Bekou, E.; Baudin, I.; Laine, J. Effect of ionic strength and hydrogen peroxide on the photocatalytic degradation of 4-chlorobenzoic acid in water. *Applied. Catalysis. B: Environmental*26 (2000) 153-171.

28. Baran, W.; Sochacka, J.; Wardas, W. Toxicity and biodegradability of sulfonamides and products of their photocatalytic degradation in aqueous solution. *Journal of Chemistry*65 (2005), 21-24.

29. Behilil, A.; Lahcene, D.; Zahraouia, B.; Benmehdi, H. ; Belhachemi, M. ; Choukchou-Braham, A. Dégradationd'un colorant cationique par la photocatalyse-solaire à travers une argileAlgérienne imprégnée avec TiO_2. *Algerian Journal of Environmental Sience and Technology* (6) 2020.

30. Azam, E.S. Photocatalytic oxidation of methylene blue dye under visible light by Ni doped Ag2S nanoparticles. *Journal of Industrial and Engineering Chemistry*20(6) (2014) 4033-4038.